Supporting Information

Brownian Diffusion of Individual Janus Nanoparticles at Water/Oil Interfaces

Dapeng Wang[1,2§*], *You-Liang Zhu*[1§], *Yuehua Zhao*[1], *Christopher Y. Li*[3], *Ashis Mukhopadhyay*[4], *Zhao-Yan Sun*[1*], *Kaloian Koynov*[2*], *Hans-Jürgen Butt*[2]

[1]State Key Laboratory of Polymer Physics and Chemistry, Changchun Institute of Applied Chemistry, Chinese Academy of Sciences, Changchun, 130022, People's Republic of China

[2]Max Planck Institute for Polymer Research, Ackermannweg 10, 55128, Mainz, Germany

[3]Department of Materials Science and Engineering, Drexel University, Philadelphia, PA 19104, USA.

[4]Department of Physics, Wayne State University, Detroit, Michigan 48201, United States

*To whom correspondence should be addressed: wdp@ciac.ac.cn; zysun@ciac.ac.cn; koynov@mpip-mainz.mpg.de;

§These authors contributed equally to this work.

Content

Materials *Page S-2*

Procedure to rule out the effect of contamination *Page S-2*

Detail of dissipative particle dynamics (DPD) simulations *Page S-2*

Effect of interfacial tension on interfacial diffusion *Page S-6*

Spatial dependent diffusion coefficient as a function of proximity to the liquid/liquid interface *Page S-8*

Contact line pinning of rough nanoparticles *Page S-9*
Figures mentioned in the main text *Page S-10*
References *Page S-11*

Materials

Alkane and water

The *n*-alkane and glycerol were purchased from Sigma-Aldrich. Water used for the sample preparation and cleaning was Milli- Q water with a resistivity of 18.2 MΩ·cm, prepared by a Sartorius Arium611VF water purification system. The purity of the alkane was promoted by a facile method as described previously [1]. The interfacial tension of water/alkane interfaces measured by a Du-Noüy ring tensiometer was listed in Table S1 and compared to literature values.

Table S1 Interfacial tension of various water/alkane interfaces (T=20°C)

***n*-alkane**	**γ (water/*n*-alkane) (mN/m) (in Ref. [2])**	**γ (water/*n*-alkane) (mN/m)**
***n*-hexane**	50.80	49.65
***n*-octane**	51.64	50.56
***n*-decane**	52.33	51.36
***n*-dodecane**	52.87	51.69
***n*-tetradecane**	-	51.93

Procedure to rule out the effect of contamination

We checked and ruled out the effect of contamination by two steps. The interfacial tension of water/alkane interfaces was consistent with the result reported previously, as shown in Table S1. Moreover, we deliberately added surfactant—sodium dodecyl sulfate into the aqueous solution at a concentration of 10^{-5}M and measured the diffusion of Janus nanoparticle at a water/decane interface. We found that the addition of the surfactant did not cause any change in $D_{||}$ within experimental uncertainty. Therefore, we concluded that the observed phenomena cannot be attributed to surface contamination.

Detail of dissipative particle dynamics (DPD) simulations

Description of DPD method

We employed a computational DPD method [3] to investigate the diffusion of nanoparticles. The DPD method was proven to be an effective mesoscopic simulation tool to study events occurring on millisecond time scales and micrometer length scales *via* tracking the motion of coarse-grained particles (composed of a group of atoms or molecules). The fundamental equation in the DPD method is Newton's equation of motion. For a particle $\boldsymbol{i}$, each DPD bead is subjected to three types of forces described as follows,

$$m_i \frac{dv_i}{dt} = \vec{F}_i = \sum_j \vec{F}_{ij}^{\,C} + \vec{F}_{ij}^{\,R} + \vec{F}_{ij}^{\,D} \quad , \tag{2}$$

where $\vec{F}_{ij}^{C}$ is the conservative force, $\vec{F}_{ij}^{R}$ is the pairwise random force, and $\vec{F}_{ij}^{D}$ is the dissipative force, respectively. The force acting on a particle is summed over all interbead forces between particles i and j. The conservative force is weakly repulsive and given by

$$\vec{F}_{ij}^{\,C} = -\nabla V(r_{ij}) = \begin{cases} \alpha_{ij}(1-\frac{r_{ij}}{r_c})\vec{e}_{ij}, & r_{ij} \le r_c \\ 0, & r_{ij} > r_c \end{cases} \quad , \tag{3}$$

where r_{ij} is the distance between particles i and j, $r_{ij} = |\vec{r}_{ij}| = |\vec{r}_i - \vec{r}_j|$, $\vec{e}_{ij} = \vec{r}_{ij}/r_{ij}$. Here, α_{ij} is a parameter to determine the magnitude of the repulsive force between particles i and j, and r_c is the cutoff distance. Random force ($\vec{F}_{ij}^{R}$) and dissipative force ($\vec{F}_{ij}^{D}$) are given by

$$\begin{aligned} \vec{F}_{ij}^{\,R} &= \sigma\omega^R(r_{ij})\xi_{ij}\vec{e}_{ij}, & r_{ij} \le r_c \\ \vec{F}_{ij}^{\,D} &= -\gamma\omega^D(r_{ij})(\vec{e}_{ij}\cdot\vec{v}_{ij})\vec{e}_{ij}, & r_{ij} \le r_c \end{aligned} \quad , \tag{4}$$

where $\vec{v}_{ij} = \vec{v}_i - \vec{v}_j$, σ is the noise parameter, γ is the friction parameter, and ζ_{ij} is the random number based on the Gaussian distribution. Here ω^R and ω^D are *r*-dependent weight functions, which are given by

$$\omega^D(r_{ij}) = \left[\omega^R(r_{ij})\right]^2 = \begin{cases} (1-\frac{r_{ij}}{r_c})^2, & r_{ij} \le r_c \\ 0, & r_{ij} > r_c \end{cases} \quad . \tag{5}$$

The temperature is controlled by a combination of dissipative and random forces. The noise parameter σ and friction parameter γ are connected to each other by the fluctuation−dissipation theorem in the following equation:

$$\sigma^2 = 2\gamma k_B T \quad , \tag{6}$$

where T is the temperature and k_B is the Boltzmann constant.

Smooth nanoparticle model

We used a single-site model to produce a smooth nanoparticle by expanding a DPD bead. The smooth nanoparticle was used to study the effect of hydrodynamic interaction near a liquid/liquid interface while phenomena of contact line pinning were eliminated. The size was tuned by a

parameter d, herein, $d = 1$ for solvent bead and $d = 5$ for the expanded nanoparticle. The conservative force is rewritten as,

$$\vec{F}_{ij}^{C} = -\nabla V(r_{ij} - \Delta) = \begin{cases} \alpha_{ij}(1 - \frac{r_{ij} - \Delta}{r_c})\hat{e}_{ij}, & r_{ij} \le r_c + \Delta \text{ and } r_{ij} \ge \Delta \\ \alpha_{ij}\hat{e}_{ij}, & r_{ij} < \Delta \\ 0, & r_{ij} > r_c \end{cases}, \quad (7)$$

where $\Delta = d_i + d_j - 1$ represents the size of nanoparticles. For two solvent beads with $d_i = d_j = 1$, then, $\Delta = 0$; the conservative force returns back to normal expression.

Coarse-grained scheme and parameters for nanoparticles that have a rough surface

For Janus nanoparticle shown in Figure S3c, two types of beads, denoted as Q and P, are stacked on a surface of each hemispheres. The parameter $\alpha_{QO} = 200$, $\alpha_{QW} = 220$, $\alpha_{PO} = 220$, and $\alpha_{PW} = 200$ were defined to allow each hemisphere to be in contact with their preferred phases. For homogeneous that had rough surface we set type Q and type P to be identical *i.e.*, $\alpha_{QO} = 200$, $\alpha_{QW} = 220$, $\alpha_{PO} = 200$, and $\alpha_{PW} = 220$, respectively.

Coarse-grained scheme and parameters for ligand-grafted nanoparticles

To mimic the ligand-grafted nanoparticles that were studied in FCS experiments, we modeled polyethylene glycol (PEG) by a hybrid scheme involving two types of DPD beads, denoted as A and B, respectively, as shown in Figure S2. The group B comprising three carbon and two oxygen atoms is more hydrophilic than group A that included four carbon and one oxygen heavy atoms. A 5 kg/mol PEG chain was modeled as a hybrid bead string which consisted of 42 beads: 28 A and 14 B. The dodecane was modeled as a string of three A beads. To model a ligand-grafted Janus nanoparticle, 60 PEG chains were grafted on one hemisphere and 60 1-dodecane chains on the other. To model a ligand-grafted homogeneous nanoparticle, 120 PEG chains were grafted uniformly on the nanoparticle surface. The beads were connected *via* harmonic springs. The spring force ($\vec{F}_{ij}^{S}$) was given by

$$\vec{F}_{ij}^{S} = -k(r_{ij} - r_0)\hat{e}_{ij} \quad (8)$$

where k is the spring constant and r_0 is the equilibrium bond distance. Harmonic spring potential with $k = 4.0$ and $r_0 = 0.0$ was utilized to describe all bond interactions. Two immiscible liquid solvents

were modeled as two types of beads, denoted as O (oil) and W (water), respectively. The core of a ligand-grafted nanoparticle consisted of 192 beads to make the nanoparticle density comparable to that of solvent matrix. The beads denoted by type G are uniformly stacked on the nanoparticle surface. The core of a nanoparticle was treated as a rigid object using the rigid body method [4]. The diameter is 5. The cutoff distance r_c is 1. The pairwise conserve force parameters α were given in Table S2. The parameters α between G beads were set as strong repulsive $\alpha = 200$ to prevent the unphysical permeation of solvent beads into the interior of a nanoparticle.

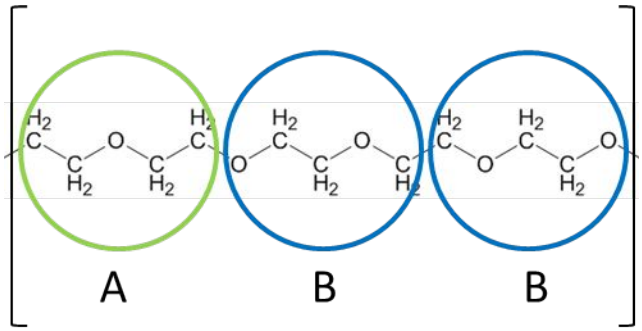

Figure S1. The schematic representation of coarse-grained bead *A* and *B* denoting five repeating units in a PEG chain.

Table S2. The conservative force parameters

α	*A*	*B*	*O*	*W*	*G*
A	25	25	25	40	200
B		25	40	25	200
O			25	80	200
W				25	200
G					25

Tuning the interfacial tension

The interfacial tension between two immiscible solvents was obtained by dividing simulation box into 100 slabs parallel to the interface and calculated according to [5]:

$$\gamma_s = \frac{1}{2}\int_{slab}[P_n(z) - P_t(z)]dz \tag{1.8}$$

The normal and transversal components of the pressure tensor $P_n(z)$ and $P_t(z)$ were calculated complying with the definition of Irving and Kirkwood [6]. Only the pairs of particles whose centers of mass connecting line passes through the infinitesimal interface should contribute to the local pressure tensor. For a planar interface, the expressions have the forms as follows,

$$P_n(z) = \rho(z)k_BT + \frac{1}{A}\left\langle \sum_{i<j} \frac{\mathbf{F}_{ij}{}^z \cdot \mathbf{r}_{ij}{}^z}{r_{ij}{}^z} \theta\left(\frac{r^z - r_i^z}{r_{ij}{}^z}\right)\theta\left(\frac{r_j{}^z - r^z}{r_{ij}{}^z}\right) \right\rangle , \tag{1.11}$$

and

$$P_t(z) = \rho(z)k_BT + \frac{1}{2A}\left\langle \sum_{i<j} \frac{\mathbf{F}_{ij}{}^x \cdot \mathbf{r}_{ij}{}^x + \mathbf{F}_{ij}{}^y \cdot \mathbf{r}_{ij}{}^y}{r_{ij}{}^z} \theta\left(\frac{r^z - r_i^z}{r_{ij}{}^z}\right)\theta\left(\frac{r_j{}^z - r^z}{r_{ij}{}^z}\right) \right\rangle . \tag{1.12}$$

Here $\rho(z)$ denotes the density at z averaged over tangential coordinates x and y and $\theta(x)$ denotes the Heaviside step function. For the term $\mathbf{F}_{ij}^{\alpha} \cdot \mathbf{r}_{ij}^{\alpha}(\alpha = x,y,z)$, we only counted the contributions of the conservative force, because our system corresponds to the correct Boltzmann distribution. We calculated the interfacial tension of two immiscible solvents W and O at three conservative force parameters $\alpha_{WO} = 60, 80, 100$. We found that the interfacial tension depended on the values of α_{WO}. The interfacial tension increases with increasing the value of α_{WO}, as shown in Figure S6. The tuning of α_{WO} was used to investigate the effect of interfacial tension on the interfacial diffusion of a Janus nanoparticle.

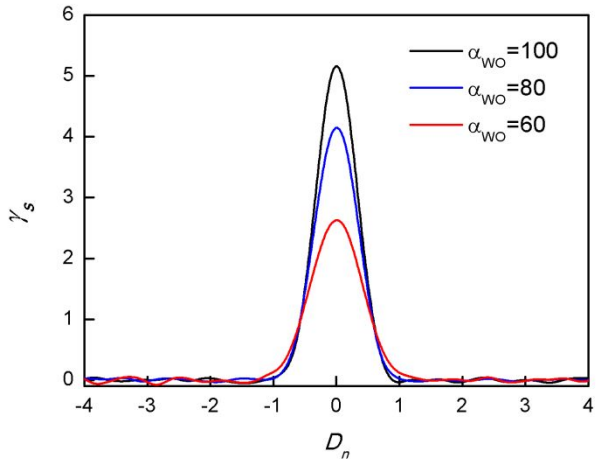

Figure S2. The interfacial tension (γ_s) as a function of the normal distance (D_n) to the interface.

Effect of interfacial tension on interfacial diffusion

According to the Einstein-Stokes relation, the interfacial tension should not play a role on diffusion. However, it is interesting to examine the effect of interfacial tension on nanoparticle interfacial diffusion. To address this issue, we performed a series of DPD simulations to study the effect of interfacial tension on diffusion of a smooth spherical particle at liquid/liquid interface. The smooth spherical particle was chosen here because we hoped to eliminate the effect of surface ligands. That allowed us to answer the question: whether the interfacial tension plays a role for interfacial diffusion of an object at a liquid/liquid interface. As expected, the variation of the interfacial tension did not change the diffusional behavior of the nanoparticle at an interface, as shown in Figure S7. These simulation results indicated that the diffusion coefficient is not as a function of the interfacial tension.

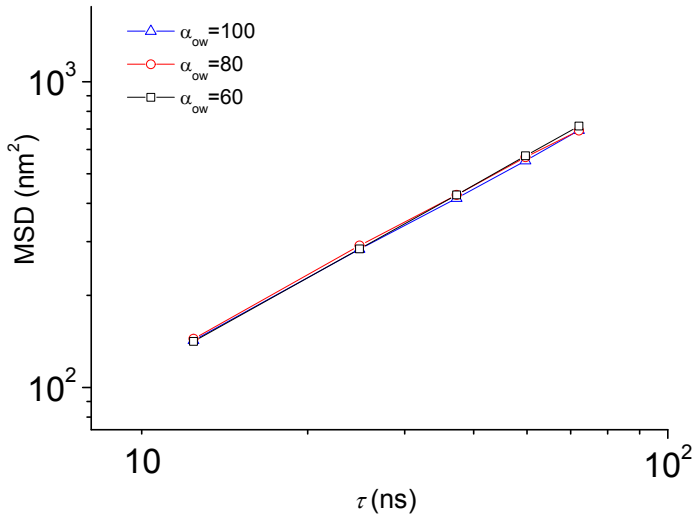

Figure S3. Mean squared displacement of a smooth nanoparticle at liquid/liquid interfaces of varying interface tension α_{ow}.

Spatial dependent diffusion coefficient as a function of proximity to the liquid/liquid interface

We first studied the effect of hydrodynamic interaction between a nanoparticle and a liquid/liquid interface. The smooth nanoparticle was initially placed in bulk and allowed to migrate to the interface. The spatial dependent diffusion coefficient was quantified as a function of proximity to the interface as shown in Figure S4. We observed a small but clear dependency of diffusion coefficient on the distance to the interface. Near the interface, diffusion coefficient was comparable

to that at the interface. These result indicated the hydrodynamic coupling between the particle and interface that resulted in slowing down of a smooth nanoparticle at a liquid/liquid interface. This leads to a decrease in $D_{DPD,||}$ relative to bulk diffusion coefficient $D_{DPD,SE}$, resulting in $D_{DPD,||}/D_{DPD,bulk}\approx 0.94$, in reasonable agreement with theoretical calculations [7].

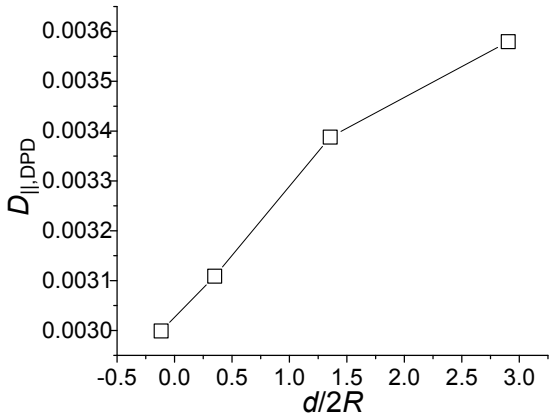

Figure S4. Spatial dependent diffusion coefficient $D_{||,DPD}$ as a function of $d/2R$ where d is the distance of the particle center to the interface and R is the radius of the particle.

Contact line pinning of rough nanoparticles

Next, we studied the effect of contact line fluctuation. Here we studied both Janus and homogeneous nanoparticles that were made from a stack of DPD beads (Figures S3b, S3c). The presence of topographic caves could act as a free energy metastable minimum to transiently lock the three-phase contact line [8]. Indeed, as shown in Figure S5, the vertical position showed transient pinning and intermetent hopping to escape from these mestastable states in an individual simulation run, consistent with previous simulation results [8]. However, this did not produce an additional random force slowing the diffusion. In this scenario, the diffusional in bulk solution and at interface is still very similar for Janus and homogeneous nanoparticles. The resulting $D_{DPD,||}/D_{DPD,bulk}$ of Janus and homogeneous NPs was 0.91 and 0.92, respectively, consistent with recent simulation results [8]. Summing up, these simulation results reflected that the contact line fluctuation is likely not the key mechanism for the anomalously slowing down of Janus nanoparticles at interfaces as observed in FCS measurments.

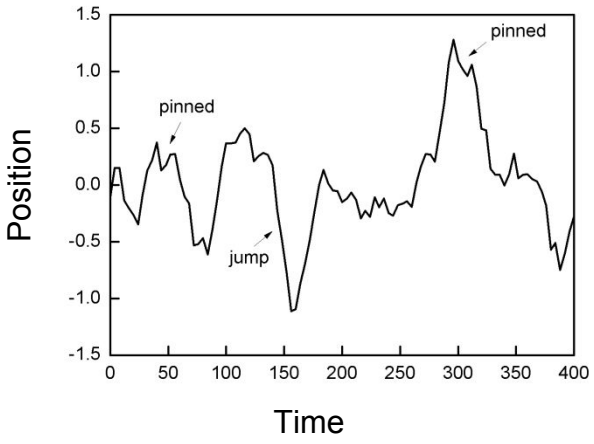

Figure S5. The vertical position of an adsorbed Janus nanoparticles at a liquid/liquid interface as a function of of time.

Figures mentioned in the main text

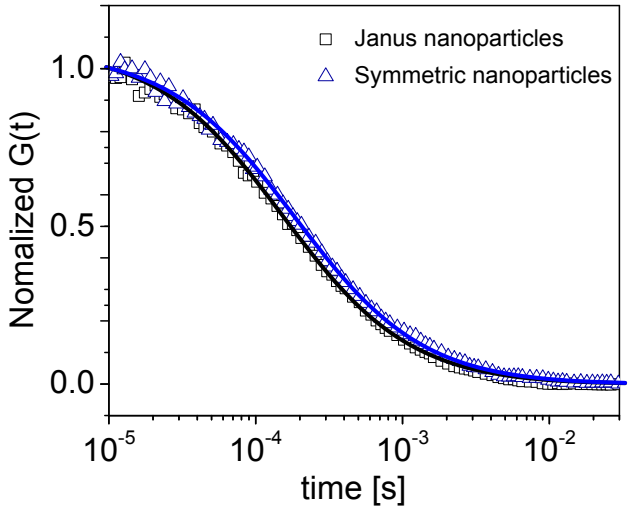

Figure S6 Normalized autocorrelation curves for Janus and homogeneous nanoparticles diffusing in bulk dichloromethane dispersion.

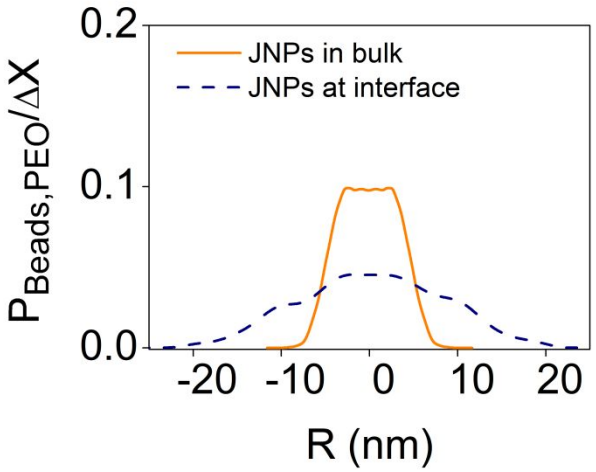

Figure S7 Normalized radial PEG density profiles for JNP in bulk water and upon adsorption at a liquid/liquid interface. In both cases the profiles are taken along the Janus boundary.

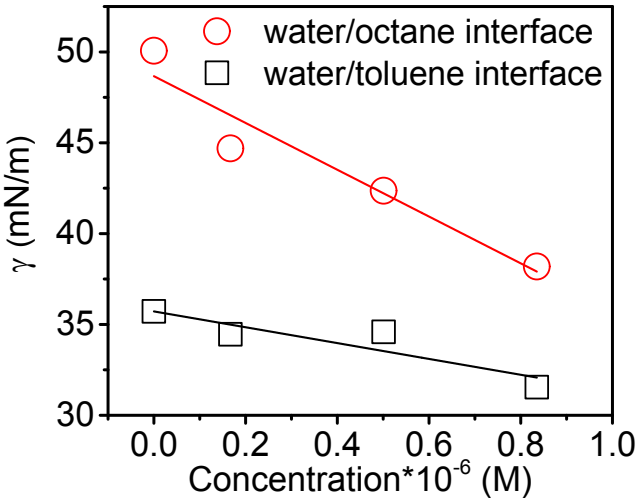

Figure S8 Equilibrated interfacial tension as a function of the bulk PEG concentration at different interfaces. The solid lines represented linear fits.

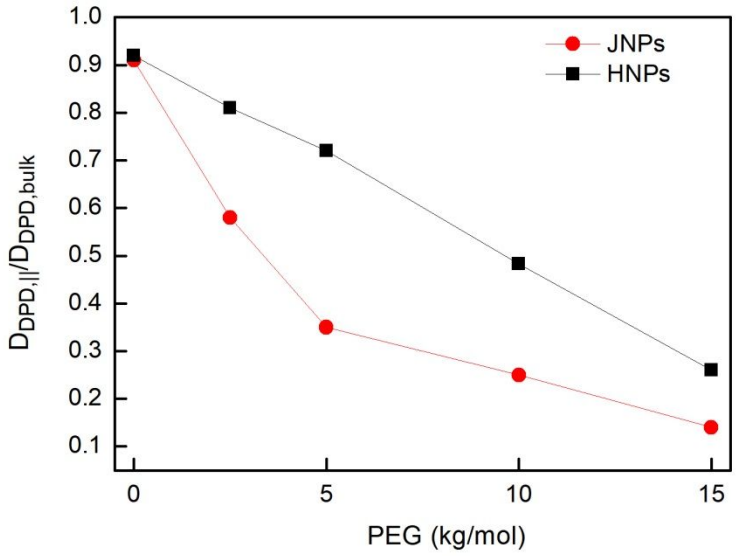

Figure S9 $D_{DPD,||}/D_{DPD,bulk}$ of JNPs and HNPs as a function of the PEG length.

References

[1] Goebel, A.; Lunkenheimer, K., Interfacial Tension of the Water/*n*-Alkane Interface. *Langmuir* **1997**, 13, 369-372.

[2] Zeppieri, S.; Rodriguez, J.; de Ramos, A. L. L., Interfacial Tension of Alkane+ Water Systems. *J. Chem. Eng. Data* **2001**, 46, 1086 -1088.

[3] Groot, R. D.; Warren, P. B., Dissipative Particle Dynamics: Bridging the Gap between Atomistic and Mesoscopic Simulation. *J. Chem. Phys.* **1997**, 107, 4423.

[4] Zhu, Y.-L.; Pan, D.; Li, Z.-W.; Liu, H.; Qian, H.-J.; Zhao, Y.; Lu, Z.-Y.; Sun, Z.-Y., Employing Multi-GPU Power for Molecular Dynamics Simulation: An Extension of GALAMOST. *Mol. Phys.* **2018**, 116, 1065-1077.

[5] Qian, H. J.; Lu, Z. Y.; Chen, L. J.; Li, Z. S.; Sun, C. C., Dissipative Particle Dynamics Study on the Interfaces in Incompatible Homopolymer Blends and with Their Block Copolymers. *J. Chem. Phys.* **2005**, 122, 184907.

[6] Irving, J. H.; Kirkwood, J. G., The Statistical Mechanical Theory of Transport Processes. IV. The Equations of Hydrodynamics. *J. Chem. Phys.* **1950**, 18, 817.

[7] Blawzdziewicz, J.; Ekiel-Jezewska, M. L.; Wajnryb E., Motion of a Spherical Particle near a Planar Fluid-Fluid Interface: The Effect of Surface Incompressibility. *J. Chem. Phys.* **2010**, 133, 114702.

[8] Koplik J.; Maldarelli, C., Molecular Dynamics Study of the Translation and Rotation of Amphiphilic Janus Nanoparticles at a Vapor-Liquid Surface. *Phys. Rev. Fluids* **2017,** 2, 044201.